

## **Modular repetitive structures as countermeasure to galloping**

\*Elena Dragomirescu<sup>1)</sup> and Yarzar Tun<sup>2)</sup>

<sup>1), 2)</sup> *Department of Civil Engineering, University of Ottawa, Ottawa K1N 6N5, Canada*  
<sup>1)</sup> [elndrag@uottawa.ca](mailto:elndrag@uottawa.ca)

### **ABSTRACT**

Wind-induced vibrations of slender high rise buildings are always an instability cause of concern. Several passive and active mitigation methods have been proposed and some of them were found to be very successful such as: dampers, wind shields and aerodynamic geometric optimization. A slender, tall sculpture entitled the Endless Column which is situated in the city of Tg. Jiu, Romania, was reported to have an extraordinary stability to wind, which might be due to its modular shape, consisting of 15 pyramidal blocks of dimensions 45 x 90 x 45 cm, plus two halves-blocks at the extremities, totaling a length of 30 m. Wind tunnel experiments performed for the aerolastic model of the Column showed that for reduced wind speeds of  $U_r = 7$  to 75 and angles of attack of  $0^\circ$ ,  $5^\circ$ ,  $10^\circ$ ,  $15^\circ$ ,  $30^\circ$  and  $45^\circ$  the Endless Column model is very stable especially at  $U_r = 75$ , where galloping was expected (Dragomirescu et al, 2009). A CFD simulation employing the LES algorithm for a model of the Column with the same dimensions as the model tested in the wind tunnel, of 1,467 cm height, 4.5 cm module's big base and 2.25 cm module's small base was performed. Pressure coefficients on 9 rings around a pyramidal module of the Endless Column were calculated and the aerodynamic coefficients, pressure contours, velocity streamlines and three-dimensional flow visualisations were recorded, for angles of attack of  $0^\circ$ ,  $10^\circ$  and  $45^\circ$  at  $Re = 2.2 \times 10^5$ . The coefficients  $C_D$  and  $C_L$  were found to be in good agreement with the experiments. The effect of the geometric shape would cause the vertical fluid motion along the Column to cancel each other, especially for the case of  $45^\circ$ , when the corners of pyramidal modules act like a wind breaker, which would confer a higher aerodynamic stability for the entire Endless Column structure.

### **1. INTRODUCTION**

The Endless Column, a famous post-modernist sculpture built out of cast iron, in Tg Jiu Romania, has proved to have an extraordinary stability to wind in spite of its slender shape composed of a vertical alignment of 15 pyramidal blocks of dimensions 45 x 90 x 45 cm, plus two halves-blocks at the extremities, totaling a height of 30 m. (Fig. 1 a).

---

<sup>1)</sup> Professor

<sup>2)</sup> Graduate Student

Several researchers have investigated the structural stability of the Endless Column and they looked at the interaction between wind flow and the Column's shape (Safta et al, 2003, Sofronie et al, 2001) or at the high mass and damping of the structure (Gabbai et al, 2007) for clarifying the "aerolastic indifference" of the Column. Column's natural frequency, distributed mass and damping were determined through in-situ measurements by Lungu et al, (2001), and wind tunnel experiments were performed, for a fixed scaled segment of 4 blocks of the Column, under laminar flow conditions for determining the aerodynamic coefficients (Solari et al, 2002). Experiments for a scaled segment of 6 pyramidal blocks (Fig. 1 b) and for a complete three-dimensional model of the Column and on a conventional square shape cylinder which were performed for comparison (Yamada et al, 2005, Dragomirescu et al, 2009), showed that the Endless Column model is very stable for high wind speeds, where the square model will encounter already galloping vibrations. However, for the lower wind speeds, the vortex induced vibrations were registered, with similar magnitudes of vibrations for both the square and the Endless Column models.



Fig. 1 The Endless Column, Tg. Jiu, Romania a) Site location (Dragomirescu et al, 2009), b) Wind Tunnel Experiment (Yamada et al, 2005)

For galloping wind induced vibrations high-rise buildings, complicated active or passive measures or control devices must be considered. The modular symmetric geometric shape could be considered as a countermeasure against galloping, if "aerolastic indifference" of the Endless Column for very high wind speeds could be completely validated. As the wind flow-structure interaction might bring some answers regarding the effect of the geometry on the wind stability a three-dimensional visualization was carried out through a CFD simulation, as none of the reported wind tunnel experiments have included a smoke visualization or a PIV test. Therefore, the current research employs an extensive 3D Computational Fluid Dynamics (CFD) simulation for elucidating the flow formation at different levels of the Endless Column and the induced aerodynamic forces.

## **2. MESH DETAILS AND SIMULATION ALGORITHM**

A rectangular simulation domain of dimensions  $5H \times 1.33H \times 1.33H$  with a model of the Column in the center of dimensions  $H = 1,467$  cm height, 4.5 cm module's big base

and 2.25 cm module's small base which corresponds to a scale of 1:20 from the prototype were considered (Fig. 2a) with a total number of 1.5 million tetrahedral cells and 250,000 nodes. The non-slip boundary condition was specified on the surfaces of the Column, and the in-flow boundary condition was set to  $u_x = 5.45$  m/s  $u_y = u_z = 0$ .

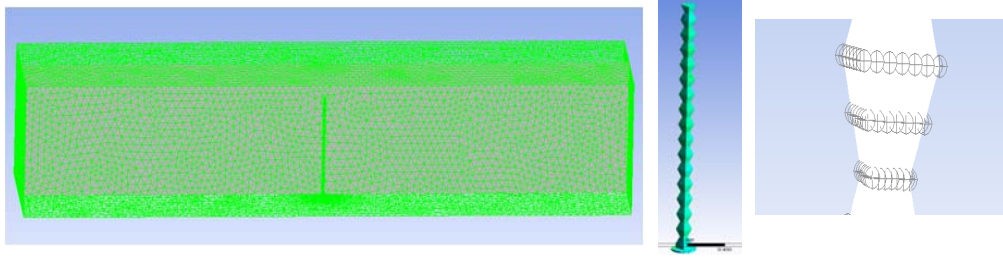


Fig. 2 CFD Simulation details (a) Mesh Characteristics, (b) Monitored rings

Pressure was monitored along two pyramidal blocks by sampling data from 9 rings around the circumference however only the middle three rings are reported here (Fig. 2 b). This arrangement will help identify the influence of the geometric shape upon the wind induced pressure and the effect the pyramidal block has on surrounding wind flow. The previous experimental investigations (Yamada et al, 2005) have shown a better response of the column for  $45^\circ$  and a slight vibration for  $0^\circ$  and  $10^\circ$ , starting at a wind speed of 5.45 m/s. Hence, these three wind angles of attack were investigated herewith, namely  $\alpha = 0^\circ, 10^\circ$  and  $45^\circ$ .

The large eddy simulation (LES) with the Smagorinsky subgrid-scale model was employed for the CFD simulation. The three dimensional incompressible Navier-Stokes equation and the equation of continuity in non-dimensional form are:

$$\frac{\partial u_i}{\partial t} + u_j \frac{\partial u_i}{\partial x_j} = -\frac{\partial P}{\partial x_i} + 2 \frac{\partial}{\partial x_i} \left( \frac{1}{\text{Re}} + \nu_{sgs} \right) D_{ij} \quad (1)$$

$$\frac{\partial u_i}{\partial x_i} = 0 \quad (2)$$

where  $u_i$  is the velocity component of grid-scale, and  $P$  is the sum of the grid-scale pressure and the residual stress.  $D_{ij}$  in Eq. (1) is the strain-rate tensor on the grid-scale velocity components:

$$D_{ij} = \frac{1}{2} \left( \frac{\partial u_i}{\partial x_j} + \frac{\partial u_j}{\partial x_i} \right) \quad (3)$$

The subgrid-scale eddy-viscosity,  $\nu_{sgs}$ , in Eq. (1) is expressed as:

$$\nu_{sgs} = (C_s \Delta)^2 \sqrt{2 D_{ij} D_{ij}} \quad (4)$$

where  $\Delta$  is the filter width and was given as the cubic-root of grid volume and the  $C_s$ , Smagorinsky constant, was set to 0.1 in this study. The invicid flux vector was determined by a standard upwind, flux-difference splitting through the low-diffusion Roe approach. For estimation of the secondary diffusion terms and velocity derivatives, the least square cell based spatial discretization was used and Third-Order MUSCL equation was considered for the flow density-based solver. The time step was chosen as  $t = 0.003$  s; pressures along the entire surface of the model was integrated, and lift

and drag aerodynamic forces were determined. More convenient, drag and lift coefficients  $C_D$ ,  $C_L$ , were extracted from the definition formulas below (Simiu and Scanlan, 1996):

$$F_D = \frac{1}{2}\rho U^2 B C_D \quad \text{and} \quad F_L = \frac{1}{2}\rho U^2 B C_L \quad (5)$$

Where  $F_D$ ,  $F_L$  are the drag and lift aerodynamic forces,  $\rho$  is density of air,  $U$  is wind speed upstream from the model deck and  $B$  is the nominal diameter of the Column's model.

### 3. CFD SIMULATION VALIDATION WITH WIND TUNNEL RESULTS

The drag and lift coefficients  $C_D$  and  $C_L$ , obtained from the numerical simulation were compared with the results obtained from the experiments performed by Solari et al, (2000), and with those performed by Dragomirescu et al, (2009), as shown in figures 3 a) and b) and were found to be in very good agreement. The highest lift force coefficient was noticed at  $10^\circ$ , as also indicated by the wind tunnel experiments, while the drag force coefficient would be highest for  $45^\circ$ . For  $0^\circ$  both aerodynamic forces were within moderate limits. In spite of the average values of the aerodynamic forces, the experiments (Yamada et al, 2005, Dragomirescu et al, 2009) have shown that if the Column is allowed to vibrate in smooth flow, the highest across-wind vibrations for 5.45 m/s are registered for  $\alpha = 10^\circ$  followed by  $\alpha = 45^\circ$ . It should be mentioned that the same experiments have revealed that a square column tested under the same conditions would have four times higher vibration amplitude.

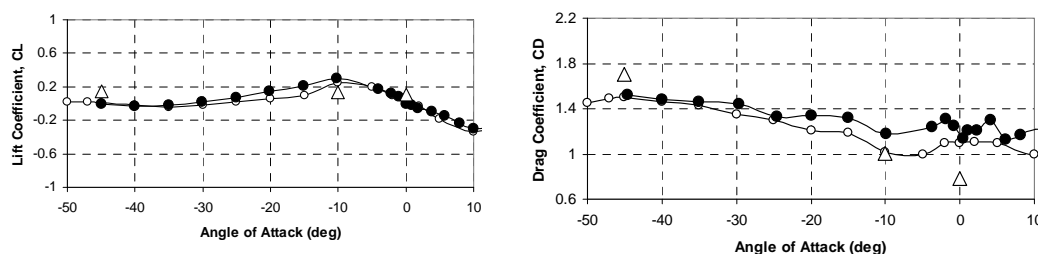


Fig. 3 Variation of aerodynamic coefficients with the angle of attack: (a) Lift Coefficient,  $C_L$ , (b) Drag Coefficient,  $C_D$

In order to determine the effect of the geometry pressure distribution on the front and back surfaces of the Column and the pressure coefficients for the monitored rings around one pyramidal block were extracted.

Non-dimensional pressure coefficients were monitored at 24 points along three rings for  $0^\circ$ ,  $10^\circ$  and  $45^\circ$  angles of attack, as shown in Figure 4. For all angles of attack, the high pressure coefficient of  $C_P = 1.0$  represents the incoming flow, or the flow reattaching to the structure. In general, from the edges of the Column the flow detaches and creates a sudden decrease in pressure coefficient, towards negative values, on the rear side of the Column, of up to  $C_P = -1.3$ . For  $0^\circ$ , after the impact with the front surface of the structure, the flow detached but the second peak indicates that a flow reattachment

occurred immediately after (Fig 4a). Similar pattern was noticed for 10°, however for the smallest line of the module (Ring1), the flow transiting was smoother than the biggest line of the module (Ring3) showing that the wind flow remains in the vicinity of the structure longer around the crest of the pyramidal blocks. The pressure coefficient had a symmetric evolution for 45°, with a clear delimitation between the pressure on the front face of the Column and the suction created by the detaching flow on the back surface of the model.

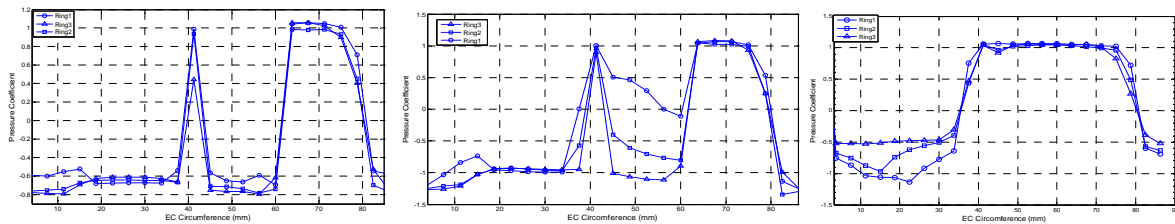


Fig. 4 Pressure distribution on the EC module at  $Re\ 2.2 \times 10^5$  on a) 0° b) 10° c) 45°

The instantaneous pressure distribution at the surface of the Column showed that for 0°, the pressure varied between 19 Pa, on the front side of the Column, where the incoming flow directly hits the structure, and a suction of -25 Pa on the downstream surface of the Column (Figs. 5 a) and b)), however the positive spike in averaged pressure coefficients in the Fig. 4 a could not be identified. The pressure on the lateral surfaces of the Column registered a higher variation. For 45° a smoother transition was noticed between the positive pressure on the front surface of the model towards the suction of up to -20 Pa registered on the downstream surface where however the distribution was not perfectly symmetric along the Column. No significant difference was noticed between the flow acting on the crest and on the trough of the module (Figs. 6 a) and b)). The main difference between the 0° and 45° was found in the highly fluctuating suction registered on the lateral faces for 0°, especially around the troughs while for 45° the evolution of the pressure on the back surface is dominated by the corner position of the Column which acts like a wind breaker, finally concluding in a much lower suction.

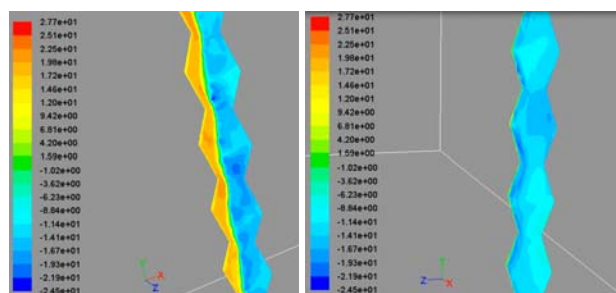


Fig. 5 Pressure distribution for 0° at  $Re\ 2.2 \times 10^5$  on a) Front and lateral surfaces b) Back surface

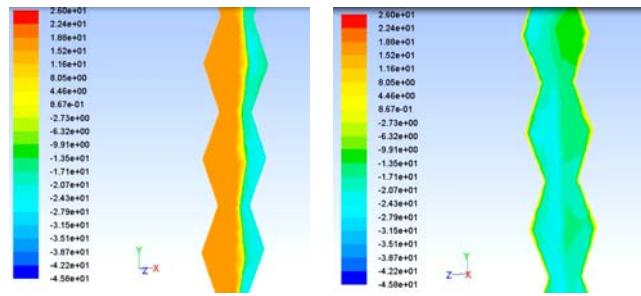


Fig. 6 Pressure distribution for 45° at  $Re\ 2.2 \times 10^5$  on a) Front and lateral surfaces b) Back surface

Several wind tunnel tests (Solari et al, 2000, Yamada et al, 2005) have attested that the particular shape of the Endless Column can provide a better stability against galloping vibrations at high wind speeds, when compared with a standard rectangular cylinder, however when an explanation is attempted, most of the aerodynamic theories consider the cross section as a reference nominal area and in this case the cross section of the Endless Column reduces to a basic square shape, for which aerodynamic characteristics are much below the structural capacities of the Endless Column. Hence, besides the pressure and aerodynamic coefficients data, more detailed three-dimensional flow visualization of the wind flow structure interaction is provided in the following section.

#### 4. FLOW-STRUCTURE INTERACTION

Velocity streamlines were sampled along sections perpendicular to the model for trough and the crest regions of the pyramidal module, similar to smoke visualization technique used in the experiments. For  $\alpha = 0^\circ$ , when the front side of the modules is facing the incoming wind flow the streamlines are deviated for both regions the crest and the trough of the pyramidal block, but they still preserve the linear pattern and no turbulence is noticed downstream the Column, as it can be seen in Fig. 7 a). For 45°, when the corner of the Column is facing the incoming flow, the streamlines are wider deviated and they tend to flow parallel to each other, without intersecting downstream the Column (Fig. 7 c)). For the case of 10°, the impact with the modules will accelerate slightly the lateral velocity streamlines and also around the trough of the module the

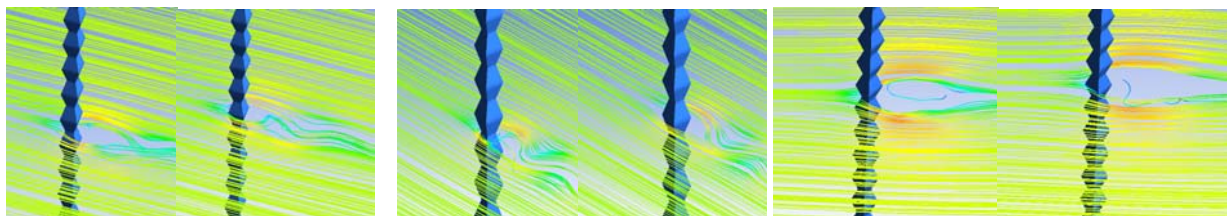


Figure 7: Pressure distribution around the Endless Column for (a)  $\alpha = 0^\circ$ , (b)  $\alpha = 10^\circ$  and (c)  $\alpha = 45^\circ$ .

streamlines will reattach on the downstream surface of the Column and will be redirected downwards along its height (Fig. 7 b)). In order to clarify the direction of the flow along the height of the Column and the possible vortex flow formations around the model, the velocity curl vectors and the three-dimensional plumes around the model are extracted. In Figs. 8 a), b), and c), the velocity curl vectors indicating the rotation axis and the sense given by the right-hand rule for each rotational flow formation, are shown for  $0^\circ$ ,  $10^\circ$  and  $45^\circ$ . It was noticed that for all the cases, on the edges of the Column, the vectors will have opposite senses, hence creating vertical motions along the height, but in opposite directions. The rotational formations have stronger vector intensity on back surface of the Column, and they are more concentrated in the troughs of the module especially for the cases of  $0^\circ$  and  $10^\circ$ . For  $45^\circ$ , lower intensity of the rotational flow formations was recorded, and the opposite curl vectors indicate the existence of vortices along the edges, where detachment is encountered.

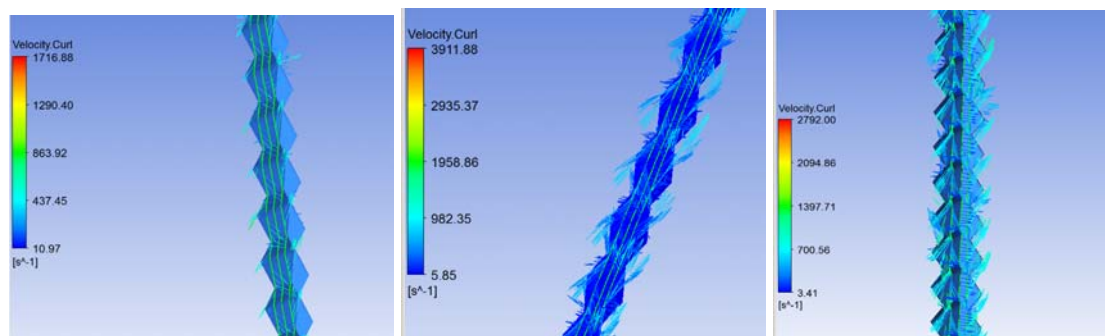


Fig. 8 Velocity curl vectors at  $Re\ 2.2 \times 10^5$  for a)  $0^\circ$  b)  $10^\circ$  c)  $45^\circ$

In Figures 9 three-dimensional flow formation around the entire Column are shown. For  $\alpha = 0^\circ$ , well defined three-dimensional turbulent formations are shed from both edges of the structure, and vertical flow formations travel downstream the Column (Fig. 9a)). A detailed image of the back surface of the Column shows the vertical flows enveloping the model, however the surface itself is not covered by this flow. The vertical three-dimensional turbulent formation is more developed for downstream the Column at  $\alpha = 10^\circ$  (Fig. 9 b)), where several vortices are formed downstream the Column. The back surface of the Column has more attached flow from the edges, but it is not completely covered indicating that most of the turbulent flow formations would be formed downstream and would not directly affect the pressure at the surface of the model. For  $\alpha = 45^\circ$  there was only one single vertical vortex behind the Column instead of several shed vortices as for  $10^\circ$ , and the detail of the back surface shows a smooth flow around the modules, however the middle corner of the back surface is not affected by the surrounding flow.

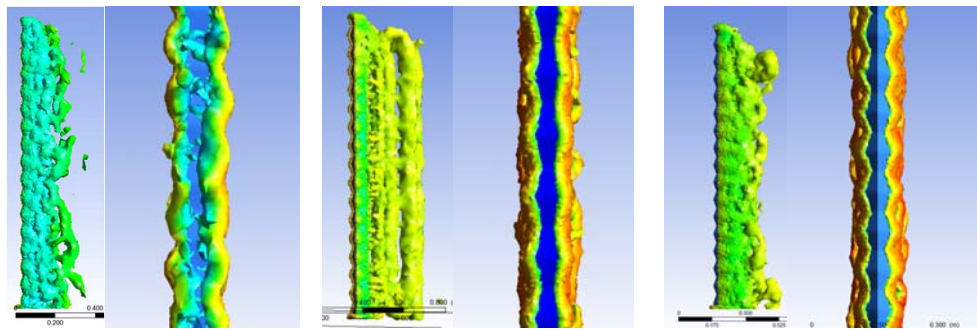


Figure 9: Three-dimensional flow formation around the Endless Column for (a)  $\alpha = 0^\circ$ , (b)  $\alpha = 10^\circ$  and (c)  $\alpha = 45^\circ$ .

Finally, sampling pressure along a middle vertical line on the front and back surfaces of the Endless Column, showed a pressure fluctuation which is consistent with the geometry of each pyramidal module, more uniform for  $45^\circ$  than for  $0^\circ$  and  $10^\circ$ , on the front face (Fig. 10 a)). The pressure measured on the exterior back surface of the modules registered values of up to  $-24\text{Pa}$  for  $10^\circ$  and up to  $-20\text{ Pa}$  and  $-16\text{ Pa}$  for  $0^\circ$  and  $45^\circ$  respectively, as it can be seen in Fig. 10 b). The vertical pressure distribution for  $10^\circ$  clearly showed the vertical vortex formed on the rear side of the Column had an average pressure of  $-19\text{ Pa}$  and only localized peaks of  $-24\text{ Pa}$ , as mentioned above.

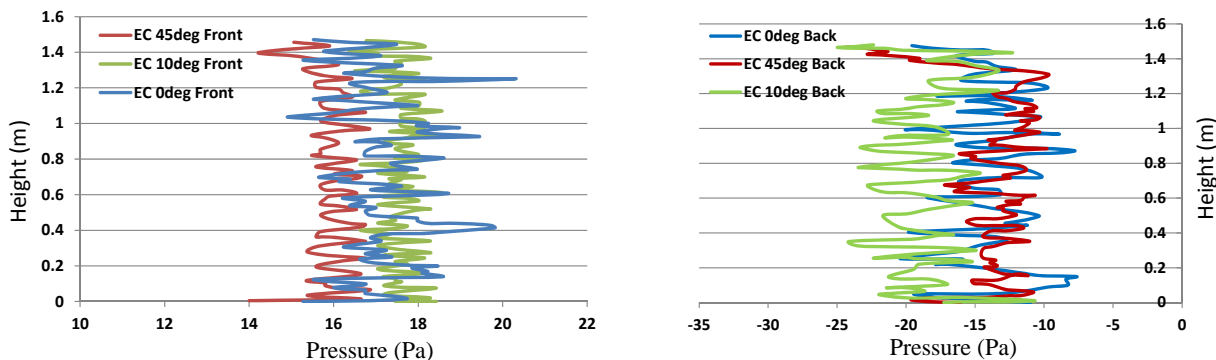


Fig. 10 Instantaneous pressure on the height of the Endless Column, for (a) Front surface, (b) Back surface

In general, the case of  $\alpha = 45^\circ$ , was the most stable in terms of pressure distribution on the vertical wind directions, the middle lines for the incoming-wind direction registering smaller pressures of around  $16\text{ Pa}$  due to the minimum nominal area exposed to wind, and also this had a very limited fluctuation along the modules.

## CONCLUSION

In an attempt of clarifying the extraordinary stability to wind of the structure Endless Column, three-dimensional flow visualization were performed by the use of CFD

simulations. Special attention was given for the details of the flow patterns around the modular shape of the Column as this was considered as being the cause of the stability to galloping, when experimentally compared with a standard square cylinder (Solari et al, 2000, Yamada et al, 2005). The dimensions of the simulated model, the wind speed and angle of attack were chosen in conformity with the wind tunnel experiments reported by Dragomirescu et al, 2009.

The effect of the geometric shape of one pyramidal module was investigated and was determined that the crest regions of the module would have less influence upon the aerodynamic activity, while the trough regions would establish a continuous accumulation of suction on the back surface of the Column. The velocity streamlines, pressure contours and vertical flow formations confirmed the fact that the most stable case is the 45° when the corners of the modules act like a wind breaker, while the critical case can be considered for 10° where pressure data and flow patterns show a more complex turbulent vertical formation on the downstream face of the Column. The negative pressure will determine an unbalanced lift force which might explain the incipient vibrations reported by the wind tunnel experiments (Yamada et al, 2005, Dragomirescu et al, 2009). Also it was noticed that the vertical fluid motions developed on both edges of the Column, for all investigated angles of attack, indicated by the opposite sense of the curl vectors.

## REFERENCES

- Blevins, R.D., (1990), "Flow-induced vibrations", *Van Nostrand Reinhold*, New York.
- Berman, P.W., Luo, S.C., (1988), "Investigation of the aerodynamic instability of a square-section cylinder by forced oscillation", *Journal of Fluids and Structures* **2**, 161-176.
- Dragomirescu, E., Yamada, H. and Katsuchi, H., 2009, Experimental investigation of the aerodynamic stability of the "Endless Column", Romania, *Journal of Wind Engineering and Industrial Aerodynamics*, **97**, 475–484.
- Gabbai, R.D., (2007), "On the aerolastic indifference of Brancusi's Endless Column", in: *Proc. of 12th Intl. Conf. on Wind Eng.*, Cairns Australia, 1111-1118.
- Kawai, H., (1992), "Vortex induced vibration of tall buildings", *J. Wind Eng. Ind. Aerodyn.*, **41-44**: 117-128.
- Klamo, J.T., Leonard, A., Roshko, A., (2006), "The effects of damping on the amplitude and frequency response of a freely vibrating cylinder in cross-flow", *J. Fluids and Struct.* **22**, 845 - 856
- Lungu, D., Solari, G., Bartoli, G., Righi, M., Vacareanu, R., Aldea, A., (2002), "Reliability under wind loads of the Brancusi Endless Column, Romania". *Intl. J. of Fluid Mechanics Research* **29**, 323-328.
- Safta, C.A., (2003), "Aerolastic Indifference of the Endless Column", *Proc. of 28<sup>th</sup> Congress of American – Romanian Academy*, Targul Jiu, Romania, 42 – 49.
- Simiu E., Scanlan R.H, (1996), "Wind effects on structures: An introduction to wind engineering", *John Wiley & Sons*, New York.
- Sofronie, R., (2001), "Brancusi and the obsession of gravity" *Proc. of Intl. Congress of ICOMOS and UNESCO*, Paris, France, 4 – 14.

Solari, G., Lungu, D., Bartoli, G., Righi, M., Vacareanu, R., Villa, A., (2002), "Brancusi Endless Column, Romania: Dynamic response and reliability under wind loading", *Proc. of the 2nd Intl Symp on Wind and Structures*, Pusan, Korea, 79-86.

Scruton, C., (1963), "On the wind excited oscillations of stacks, towers and masts", *Proc. Intl. Conf. of Wind Effects on Buildings and Structures*, Teddington, U.K., 798-836.

Yamada, H., Katsuchi, H., Dragomirescu, E., Takaoka, Y., (2005), "Wind-tunnel study on aerodynamics of Endless-Column", *Proc. of Conf. of Wind Eng.*, Tokyo, Japan, 45 – 48.